Electron localization in Ge/Si heterostructures with double quantum dots detected by an electron spin resonance method

A. F. Zinovieva,[*] A. I. Nikiforov, V. A. Timofeev, A. V. Nenashev, and A. V. Dvurechenskii

Institute of Semiconductor Physics, SB RAS, 630090 Novosibirsk, Russia

L. V. Kulik

Institute of Chemical Kinetics and Combustion, SB RAS, 630090 Novosibirsk, Russia

Electron states in Ge/Si heterostructures with double quantum dots were studied by use of the electron spin resonance (ESR) method. It was demonstrated that the spatial localization of electrons as well as the localization in the momentum space can be controlled by the change of spacer thickness between quantum dots layers. New ESR signals, indicating the electron localization on the base edges of quantum dots, were obtained for the structures with the double layers of vertically aligned Ge quantum dots separated by a 2-nm-thick Si layer. Anisotropy of the g factor is typical for electron states in Δ^{100} and $\Delta^{\bar{1}00}$ valleys. Strain distribution in the structures under study makes the localization of electrons in these valleys at the base edges of quantum dots energetically favorable. The broadening of the ESR line due to electron-hole exchange interaction was detected. Theoretical estimation of the exchange interaction magnitude based on the experimental data gives $J \approx 0.1~\mu$eV.

I. INTRODUCTION

Quantum computation ideas inspires the researchers in all world to seek new ways and systems for the creation of the basic elements for quantum calculations. Intensive studies are carried out in directions of qubit realization on the base of the polarization state of a photon, states of trapped atoms and ions, nuclear spins in molecules in liquid solutions, spin or charge states in quantum dots (QDs) and dopants in solids and on the base of superconducting circuits.[1,2] One of the main parameters showing the applicability of system for quantum computation is the spin coherence time. An extremely long spin lifetime is expected in zero-dimensional structures based on Si due to weak spin-orbit (SO) coupling in this material. In Ge/Si system with self-assembled QDs electrons are localized in strained Si regions near Ge QDs and have potential for long coherence time. However, the organization of quantum calculations needs the tunneling coupling between electron states. The natural way of creating the QDs with sufficient tunneling coupling is the growth of stacking QDs with vertical alignment and small width of separating layers. In these structures the strain distribution has a great influence on the energy spectrum of electrons localized near the QDs. Strain accumulation in a fourfold SiGe QD stack was used to increase the binding energy of electrons localized near QD apexes.[3] Yakimov *et al.*[3] succeeded in creating QD structures with a binding energy of electrons of approximately 60 meV. In recent work[4] the possibility of ensemble single-qubit operations on electrons localized on the apexes of SiGe quantum dots was demonstrated in pulsed electron paramagnetic resonance (EPR) experiments. However, for quantum calculations it needs selective access to individual qubits for implementation of one-qubit and two-qubit operations (for example, the controlled-NOT gate or combinations of single-spin rotations of two coupled electrons and the SWAP gate). From this point of view it will be better to distinguish these electrons in the g-factor value to perform separate single-spin rotations.

Strain in the SiGe QD system can be used to obtain effective localization of electrons with different g factors. Earlier, in classical work, D. K. Wilson and G. Feher[5] demonstrated the effect of uniaxial strain on the g-factor value in ESR experiments on donors in silicon. In this work the samples were subjected to external uniaxial stresses (strain was one order with 10^{-3}), resulting in g shift $g - g_0$ of the order of 10^{-4} due to the effect of the strain-induced valleys repopulation. Internal strain in the SiGe QD heterosystem is one order larger, which allows us to obtain only two Δ-valley populations (for example, Δ^{001} and $\Delta^{00\bar{1}}$) and the highest possible in this heterosystem g-factor difference $\delta g = 1.1 \times 10^{-3}$ (Ref. 6). Such a large g-factor anisotropy has been obtained in recent ESR experiments[6] on GeSi QD structures with localization of electrons near the apexes of QDs, corresponding to the localization of electrons in Δ^{001} and $\Delta^{00\bar{1}}$ valleys.

Inhomogeneous strain distribution in Si surroundings of Ge QDs can lead to the formation of potential wells for electrons not only near the QD apexes but in other Si regions surrounding Ge QDs. In a recent work[7] it was shown theoretically that the strain in stacked QD structures with eight QD layers induces the formation of the deep potential well near the base edge of QDs where the localization of electrons in Δ^{100} and $\Delta^{\bar{1}00}$ valleys is possible. At special parameters of the structure the depth of this potential well can be deeper than the depth of potential well near the apex of QD. These results open the possible way of electron localization in Δ^{100} and $\Delta^{\bar{1}00}$ valleys through the governing of the strain distribution in stacked QD structures. The localization of electrons in these Δ valleys can provide another g-factor value of electrons and makes possible the single- and two-qubit operation implementation in the future.

In the present work the possibility of localization of electrons with different g factors in the Ge/Si QD system was demonstrated. ESR measurements of Ge/Si heterostructures with double quantum dots show that the place of electron localization can be controlled by the change of the spacer

thickness between QD layers. Different spatial localization of electrons leads to different *g* factors. These results can be used in the future for the building blocks of a quantum computer.

II. STRAIN AND ELECTRON LOCALIZATION IN GESI QD SYSTEM

Let us consider all places of possible localization of electrons in GeSi system with Ge QDs. First, the typical shape and sizes of Ge QDs should be described, since these parameters have a great influence on the strain distribution in a surrounding Si matrix. Usually Ge QDs are grown by conventional molecular beam epitaxy on Si(001) substrates and can have the shape of square pyramids, elongated hut clusters, and dome clusters.[8] Change of QD shape accompanies an increase of QD size. Small pyramids arising at earlier stages of epitaxy have typical lateral sizes of 10–20 nm and heights of 1–2 nm. Elongated hut clusters have a short base edge size of 10–20 nm, while the size of the long base edge can increase up to 40–50 nm; at that size the height of QD remains near 1–2 nm. The typical sizes of dome clusters are 50 nm in the lateral direction and 10 nm in height. Dome clusters can induce the largest strain in the Si matrix and provide the electron localization in Si surroundings with the largest binding energy. However, this type of QD is grown at higher temperatures ($\sim$600 °C), and GeSi intermixing, as well as a high probability of dislocation introduction, can lead to the loss of the above-mentioned advantages. Therefore we do not consider dome clusters further. As concerning pyramids and hut clusters, there is one more important parameter which can affect the symmetry of the *g* tensor for electrons localized on QD. This is an orientation of QD edges in relation to crystallographic directions. The square pyramids and hut clusters have the base edges oriented along the [100] and [010] directions. Additionally, hut clusters during growth can be elongated in these directions with equal probability; approximately half of the nanoclusters are oriented in the [100] direction and half of the nanoclusters have the [010] orientation.

The first and main place of localization is the Si region close to the apex of the Ge quantum dot (see Fig. 1). The strain in this region is close to an effective uniaxial compression along the growth direction of structure *Z* and an in-plane tension.[9] These strains cause a splitting of the sixfold-degenerate Δ valley and a separation of the two lower Δ^{001} and $\Delta^{00\bar{1}}$ valleys and of the four upper in-plane Δ valleys. The localized electron state (a green cloud in Fig. 1) is formed by states of two lower Δ valleys. The symmetry of the *g* tensor of this electron state is defined by the symmetry of the isoenergetic surface (an ellipsoid of revolution). When the external magnetic field **H** is applied parallel to the ellipsoid axis, the ESR signal with a pure $g_\parallel$ value is observed, and when **H** is perpendicular to this axis, the ESR signal with $g_\perp$ is measured.[6] The same picture can be observed for electrons localized in a potential well under the bottom of the Ge quantum dot, where the strain distribution is similar.

Another possible place of electron localization is the region close to the base edges of the QDs.[10] But this electron state (a red cloud in Fig. 1) is found to have a higher energy than the
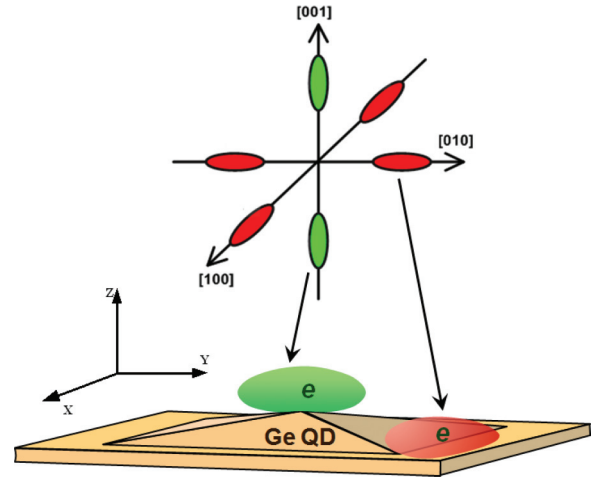

FIG. 1. (Color online) Scheme of possible electron localization places in the vicinity of Ge quantum dot.

electrons localized at the apex of the QDs. For example, the theoretical calculation of the energy spectrum for electrons in three-dimensional QD crystals with pyramidal QDs with a base size of $l = 35$ nm and height $h = 3$ nm gives a binding energy for electrons localized at the QD base edge that is smaller by approximately 50 meV than the binding energy of electrons at the apex of the QD ($E_{\Delta xy} = 1158$ meV, $E_{\Delta z} = 1105$ meV; the origin of the energy scale is the average point of the three valence bands in unstrained Si). It should be noted that for small quantum dots (typical hut clusters with a base size of $l = 15$ nm and height of $h = 1.5$ nm) electrons cannot localize at the base edges of the QDs, because the corresponding potential well is narrow. The localization becomes sufficient with the base size close to $l \approx 30$ nm.

The strain distribution in the Si region near the center of the base edge of QD is close to the following: for base edges directed along the [100] direction there is tension along the [100] direction and compression along the [010] direction. This leads to analogous splitting of the Δ valley, only in this case the lower valleys will be the Δ^{010} and $\Delta^{0\bar{1}0}$ valleys. Such a disposition of the Δ valleys can lead to another orientation dependence of *g* factor of the QD electron. When the external magnetic field **H** is applied parallel to the growth direction of the structure [001], the pure $g_\perp$ value should be observed, and for the in-plane magnetic field the *g* factor value is defined by the angle φ between the magnetic field and the major valley axis along [010] direction as follows:

$$g^2 = g_\parallel^2 \cos^2(\varphi) + g_\perp^2 \sin^2(\varphi). \tag{1}$$

The consideration of another QD base edge along the [010] direction gives a similar picture, but in this case the *g*-factor values will be governed by symmetry of lower Δ^{100} and $\Delta^{\bar{1}00}$ valleys. In experiments electrons are localized with equal probability at the base edges along the [010] and [100] directions, and then two ESR lines should be observed for the in-plane magnetic field. For example, for an in-plane magnetic field applied along the [100] direction one ESR line will have a *g* factor $g = g_\perp$ and the second ESR line will have $g = g_\parallel$. However, if we apply the magnetic field along the [110] direction, we will observe the single ESR line with the

g factor defined by Eq. (1) with $\varphi = 45°$, since all electrons localized at the base edges of the QDs will have one g factor $g_{xy} = \sqrt{1/2 g_\parallel^2 + 1/2 g_\perp^2}$, where $g_\parallel$ and $g_\perp$ are the longitudinal and transversal components of the electron g tensor in bulk Si.[11]

So there is a principal possibility of localization of electrons with different g factors in Ge/Si system with quantum dots. Electron localization near the apex of Ge QD was proved by ESR measurements and an analysis of g factor angular dependence in the Ref. 6. The question about localization near base edges of Ge QDs remains open until now.

III. SAMPLE AND EXPERIMENT

Samples were grown by molecular-beam epitaxy on n-Si(001) substrates with a resistivity of 1000 Ω cm. We have grown 5 double layers of QDs separating by 30-nm-thick Si layers. To find the optimal conditions for localization of electrons in Δ^{100} and $\Delta^{\bar{1}00}$ valleys, QD structures with varied spacer distance d from 2 to 4 nm were created. Each QD layer was formed by deposition of 5 ML Ge at the temperature $T = 500\,°C$. On the top of the structure, a 0.3-μm epitaxial n-Si layer (Sb concentration $\sim 5 \times 10^{16} cm^{-3}$) was grown, and the same layer was formed below the QD layers. It should be noted that the QD layers are not intentionally doped; nevertheless, we estimated a residual MBE background doping of about 10^{16} cm^{-3}. The scanning tunneling microscopy (STM) of the structure with one double QD layer uncovered by Si shows that the QDs have the shape of elongated hut clusters with the largest lateral size reaching $l = 40$ nm (Fig. 2). The short base side of QDs is about 10–15 nm and the height is 1–1.5 nm. The density of hut clusters is $\sim 8 \times 10^{10}$ cm^{-2}. Cross-sectional images obtained by transmission electron microscopy (TEM) show that there are no dislocations in the sample and the QDs in the double layers are vertically aligned. It is clearly seen from STM that the QDs are arranged into groups composed of a few nanoclusters. In most cases the nanoclusters in these groups are aligned along largest base edges, oriented preferentially either along $\langle 100 \rangle$ directions or along $\langle 010 \rangle$ directions. Such an arrangement of QDs turns out to provide the localization of electrons in Δ^{100} and $\Delta^{\bar{1}00}$ (Δ^{010} and $\Delta^{0\bar{1}0}$) valleys near the base edge between closely spaced aligned nanoclusters.

Calculations of the energy spectrum in the effective mass approximation (model structure shown in the Fig. 3) demonstrate that the localization at the base edge of the QDs becomes favorable at certain sizes and distances between the QDs. At least one lateral size of QD should be larger 30 nm. It needs a gap between aligned base edges, $b \approx 2$–3 nm, at zero gap the localization does not occur. Deepest electron state was obtained at vertical distance between QD layers being equal to the height of QD due to effective accumulation of strain. Calculation, using the effective mass method, with parameters $l_x = 12$ nm, $l_y = 36$ nm, $h = 1$ nm, $d = 1$ nm, $b = 3$ nm and typical Ge content $x = 0.7$, gives the energy of ground state $E_0 \approx 10$ meV for electron from Δ^{100} and $\Delta^{\bar{1}00}$ valleys, while for electrons from Δ^{001} and $\Delta^{00\bar{1}}$ valleys the energy of electron state consists of $E_b \approx 5$ meV. With increasing vertical distance up to $d = 2$ nm the state of electron
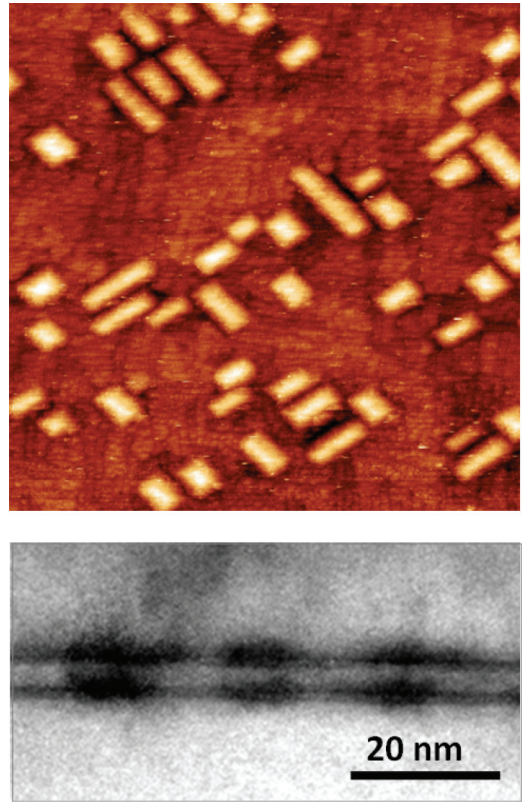

FIG. 2. (Color online) STM image (250×250 nm) of an uncovered sample with a double layer of QDs separated by a distance $d = 2$ nm in the vertical direction (top panel). TEM image of the QD double layer structure with $d = 2$ nm (bottom panel).

from Δ^{100} and $\Delta^{\bar{1}00}$ valleys remains deepest, but the binding energy decreases down to 7 meV, while the electron state corresponding to Δ^{001} and $\Delta^{00\bar{1}}$ has the energy 3 meV. To make localization of electrons stronger, we add the Coulomb interaction with ionized impurity atoms embedded in Ge QDs. In experimental structure the doping level corresponds to 1–2 Sb atoms inside Ge QDs. In this case the binding energy of electrons becomes >40 meV, which provides the effective localization of electrons on QDs in the samples doped by Sb. The hyperfine interaction with nuclear spin of the impurity located in Ge is negligible because the electron wave function does not penetrate the Ge barrier and spin properties of electron are determined by Si surroundings.

ESR measurements were performed with a Bruker Elexsys 580 X-band EPR spectrometer using a dielectric cavity Bruker ER-4118 X-MD-5. The samples with QD double layers were cut along the principal crystalline directions [110] and [$\bar{1}$10], as indicated in Fig. 4, and glued on a quartz holder, allowing a rotation of the sample in the magnetic field, and then the entire cavity and sample were maintained at low temperature ($T = 4.5$ K) with a helium flow cryostat (Oxford CF935). All g factor values were calibrated to the conduction electron g factor of Li metal particles in LiF (Ref. 12) in order to guarantee the precision of the g factor determination. In some experiments the samples are illuminated by tungsten-halogen lamp through the optical access windows in the cryostat and resonator.
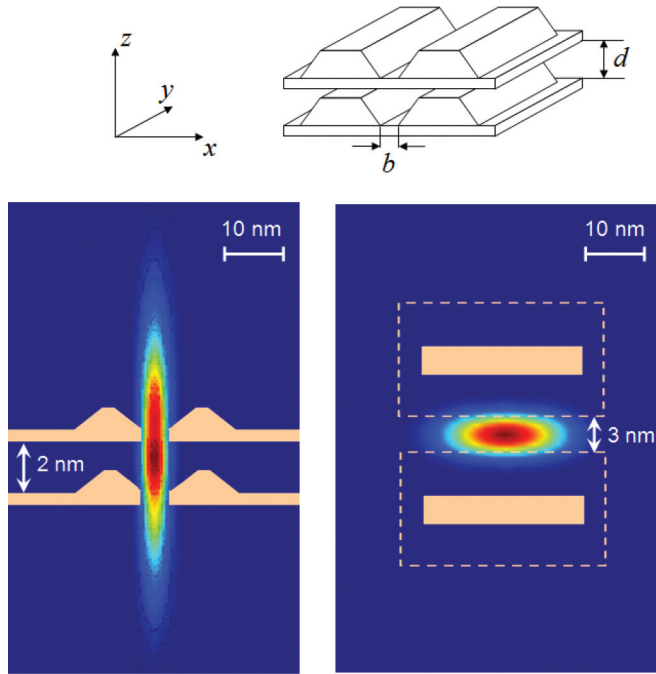
FIG. 3. (Color online) Model structure with double layer of QDs separated by distance d in the vertical direction and gap b in the horizontal direction (top panel). Wave function of the ground electron state calculated for the structure with $d = 2$ nm and $b = 3$ nm; section of the XZ plane passing through the center of the long base edge (bottom left panel); section of the XY plane passing through apexes of QDs in the lower layer (bottom right panel). Scales along different axes differ.

TABLE I. Experimental results (g factor and peak-to-peak ESR linewidth ΔH_{pp}) obtained for double QD structures with different spacer distance d. For the structure with $d = 2$ nm the results obtained with and without illumination are presented. For the structures with $d = 3$ and 4 nm, illumination does not change the ESR data. θ is the angle between the magnetic field direction and the crystallographic direction [001].

d (nm)	g factor		ΔH_{pp}, Oe	
	$\theta = 0°$	$\theta = 90°$	$\theta = 0°$	$\theta = 90°$
2 (dark)	1.9985	1.9990	1.8	1.4
2 (light)	1.9985	1.9990	2.2	1.7
3, line 1	1.9994	1.9985	1.2	1.4
3, line 2	2.0002	2.0000	2.5	1.8
4	1.9992	1.9992	1.4	1.0

IV. RESULTS AND DISCUSSION

All investigated structures demonstrated ESR signals corresponding to electrons localized in Si layers in vicinity of QDs. Experimental results are given in the Table I. Angular dependencies of g factor and ESR linewidth are obtained by rotating of magnetic field from [001] to [110] direction. Most part of ESR signals have the anisotropic g factor and ESR linewidth angular dependencies. Observed g factor anisotropy for the structures with $d = 2$ nm and $d = 3$ nm (marked as "line 1" in the Table I) can be associated with localization of electrons in strained Si regions near Ge QDs.

Very interesting behavior of ESR linewidths is observed for all structures under study. Practically all ESR lines are narrowed with the change of the magnetic field orientation from the growth direction Z to the in-plane direction. Usually for the structures with the inversion asymmetry (QD structures,[6] two-dimensional electron gas structures[13]) the opposite effect is observed: the ESR lines broaden with deviation of the magnetic field from Z. This broadening occurs due to the special in-plane arrangement of spin-orbit fields (Rashba fields), leading to anisotropy of spin relaxation processes in the system.[14] In the present study the main parameter defining the unusual orientational dependence of linewidth is the electron localization radius. This parameter in investigated structures is comparable with the magnetic length λ. Magnetic length $\lambda = \sqrt{c\hbar/eH}$ in our experimental setup ($H = 3440$ Oe) is about of 45 nm, that is very close to the size of long QD base edges (≈ 40 nm) and, correspondingly, to the size of electron wave function, elongated in this direction (see Fig. 3). In these conditions the magnetic field applied along the growth direction [001] can effectively shrink the tails of electron wave functions,[15] resulting in enhancement of electron localization. With deviation of the magnetic field from the growth direction the shrinking effect vanishes and the localization of electrons becomes weaker. This leads to more effective overlapping of wave functions of electrons localized in neighboring QDs. Increase of the overlapping can promote two possible processes leading to the narrowing of the ESR linewidth.

The first process is the electron hopping between QDs. The hopping results in the narrowing of ESR line, provided that the electron motion occurs in a restricted area, for example,
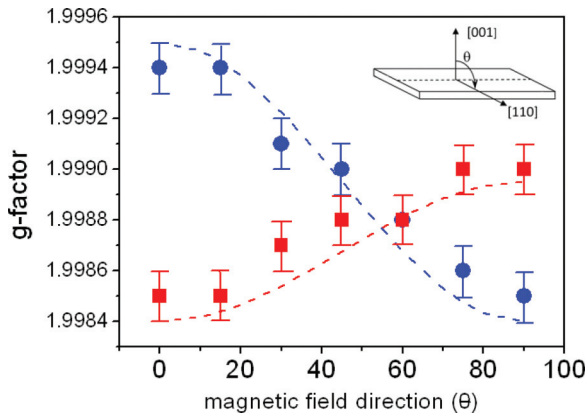

FIG. 4. (Color online) Angular dependence of the g factor for the structure with double vertically aligned Ge/Si QDs, the distance between QDs layers $d = 2$ nm (squares). Circles show the angular dependence of the g factor for one of two ESR lines (line 1) obtained for the structure with the distance $d = 3$ nm. The dashed red line presents the expected theoretical angular dependence of the g factor for electrons localized in Δ^{100} ($\Delta^{\bar{1}00}$) and Δ^{010} ($\Delta^{0\bar{1}0}$) valleys at the rotation of magnetic field from the [001] to the [110] direction. The dashed blue line presents the expected theoretical angular dependence of the g factor for electrons localized in Δ^{001} ($\Delta^{00\bar{1}}$). θ is the angle between the magnetic field direction and the crystallographic direction [001].

in some isolated groups of quantum dots.[16] In this case electrons move along the same trajectory within this group and the effective averaging of local magnetic fields induced by nuclear spins of ^{29}Si occurs. In the same way, averaging of the differences of QD parameters, such as GeSi composition and QD size, takes place. The presence of isolated groups of QDs in the samples under study is clearly seen in the STM image (Fig. 2).

The second process is the averaging through the exchange interaction between electrons in neighboring QDs. This interaction also depends on the overlapping of wave functions and becomes more intensive at the deviation of magnetic field from the Z direction. As a result, for the in-plane magnetic field the narrowest ESR lines are observed.

There is one more actor changing the ESR linewidth in our experiments. The illumination of the sample causes ESR line broadening, but only for the structure with $d = 2$ nm. For the structures with other spacer thicknesses ($d = 3$ and 4 nm) the illumination does not change the ESR linewidth.

A. Electron localization on the base edge of QD

New ESR signal, indicating the electron localization on the base edge of QD, is observed on the structure with double QD layers, separated by a distance of $d = 2$ nm. The g factor of obtained ESR signal is $g_{zz} = 1.9985 \pm 0.0001$ for a magnetic field applied along the growth direction [001]. In a perpendicular magnetic field applied along the [110] direction we have observed the ESR signal with $g_{xy} = 1.9990 \pm 0.0001$. Whole orientation dependence of the g factor is shown in Fig. 4 (red squares) for a magnetic field rotating from the [001] to the [110] direction. Such anisotropy is typical for electron states localized in Δ^{100} and $\Delta^{\bar{1}00}$ (Δ^{010} and $\Delta^{0\bar{1}0}$) valleys and can be explained by the symmetry of the isoenergetic surface (an ellipsoid of revolution) of the energetic valleys in Si (a very nice explanation can be found in the classical work of D. K. Wilson and G. Feher[5]).

ESR spectra obtained at different magnetic field orientations are shown in Fig. 5. It is clearly seen that the ESR linewidth has the nonmonotonic angular dependence. At the initial stage $\theta \in \{0° \div 30°\}$ the ESR line is narrowed from $\Delta H_{pp} \approx 1.8$ Oe down to $\Delta H_{pp} \approx 1.4$ Oe, then it broadens up to $H_{pp} \approx 1.8$ Oe ($\theta = 60°$), and, finally, the ESR line is narrowed again to $\Delta H_{pp} \approx 1.4$ Oe. The similar behavior is observed in QD structures with a large electron localization radius comparable with the magnetic length λ.[16] Such a dependence can be explained assuming that the main mechanism of spin relaxation is the spin precession in effective magnetic fields at random electron hopping between QDs (Dyakonov-Perel mechanism in the hopping regime).[17,18] Nonmonotonic behavior of ESR linewidth (see the inset in the Fig. 5) is well described in the framework of the Redfield model[19] with the hopping time depending on the magnetic field. This question is discussed in detail in Ref. 16. The ESR linewidth behavior can be understood as a result of the competition of two mechanisms. Narrowing occurs by means averaging due to the wave function extension with the deviation of the magnetic field from the growth direction. The Dyakonov-Perel mechanism is responsible for ESR line broadening.
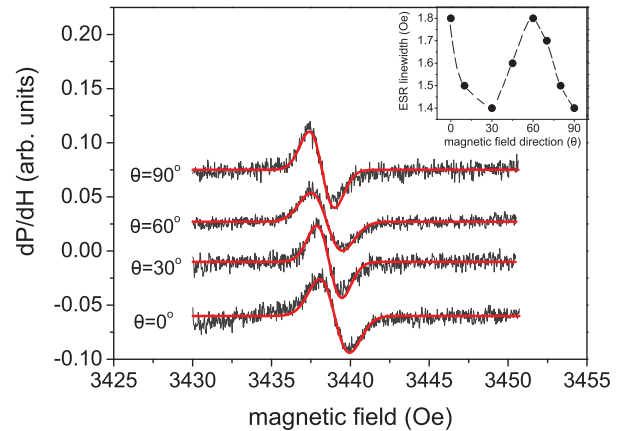

FIG. 5. (Color online) ESR spectra of electrons localized in the structure with double vertically aligned Ge/Si QDs for different sample orientation in the magnetic field; the distance between QD layers $d = 2$ nm. The magnetic field is directed along the growth direction of the nanostructure for $\theta = 0°$, $\nu = 9.61940$ GHz, $T = 4.5$ K, microwave power $P = 0.063$ mW. The inset shows the angular dependence of the ESR linewidth.

B. Broadening of the ESR line under illumination

The efficiency of electron localization can be increased by Coulomb interaction with a photogenerated hole, localized inside a double QD. This is confirmed by the increasing intensity of the ESR signal at the illumination of the sample by use of a tungsten-halogen lamp. Electron-hole pairs are generated through interband transitions, and then holes are trapped by deep potential wells inside Ge quantum dots, charging them positively. Electrons in the conduction band are attracted by positively charged quantum dots and localized in the vicinity of Ge quantum dots. The spatially indirect excitons are formed as result of illumination (electrons are localized in Si and holes are localized in Ge).[20] In the case of the sample with the single quantum dot layer the illumination could not lead to any change in the ESR linewidth, because the overlapping between the electron and hole wave functions is negligible. However, if one takes the double quantum dot (vertically aligned with spacer thickness $d = 2$ nm), one can obtain very interesting phenomena. The hole wave function is distributed between the top and bottom quantum dots, and the probability of finding the hole in the Si spacer between the QD layers becomes significant.[21] If the electron is localized in the Si spacer (as in structure with $d = 2$ nm), the overlapping of the hole and electron wave functions becomes noticeable and can be detected as a broadening of the ESR line. This effect is very sensitive to the thickness of the Si spacer and disappears when this parameter is changed. In Fig. 6 the ESR signals from electrons localized in the vicinity of QDs in the magnetic field applied along the [001] direction with and without illumination are shown. The light-induced broadening of the ESR signal is clearly seen. The ESR linewidth without illumination is equal to $\Delta H_{pp} = 1.8$ Oe, while under illumination the ESR linewidth increases up to $\Delta H_{pp} = 2.2$ Oe. The electron g factor does not change with illumination. It was verified by comparison with position of the reference ESR line (conduction electron line of Li metal
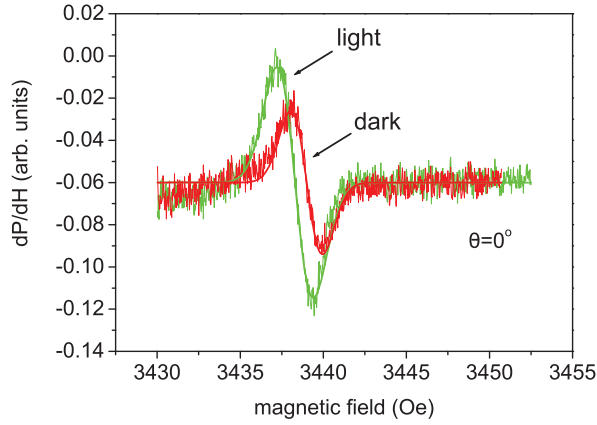
FIG. 6. (Color online) ESR spectra of electrons localized in the structure with double vertically aligned Ge/Si QDs, the distance between QDs layers $d = 2$ nm. For $\theta = 0°$ the magnetic field is directed along the growth direction of the nanostructure, $T = 4.5$ K; microwave power $P = 0.063$ mW. ESR line shifts due to the change of the resonance frequency under illumination ($\nu = 9.61940$ GHz without light, $\nu = 9.61749$ GHz with light). Electron g factor does not change with illumination.

particles in LiF). The ESR line shift that is clearly visible in Fig. 6 occurs due to the change of the resonance frequency of microwave resonator. The illumination leads to the appearance of free carriers in the sample. Some part of the electrons is not trapped by the QD layers and provides conductivity in the system. The ESR signal from these electrons has a very large linewidth (Sb doping of the epitaxial cap-layer)[22] and it is not detectable in our experimental conditions. But they can provide some change of resonance frequency.

It is quite logical to assume that the broadening of the ESR line is a result of decreasing the spin relaxation time of the electrons due to the interaction with holes. Holes localized inside Ge quantum dots have a shorter spin relaxation time due to a larger spin-orbit constant. Exchange interaction with quickly relaxed hole spins promotes the relaxation of electron spins. This interaction is described by the Hamiltonian $\hat{H} = J_{st}\vec{S}_1\vec{S}_2$; from this one can estimate the magnitude of the electron-hole exchange interaction J_{st}.

We made this estimation based on the following simple assumptions. Let the electron be found in the initial state with polarization P_e, and let the hole be unpolarized. The carriers are not entangled at the moment $t = 0$. The evolution of electron polarization can be described by the following expression:

$$P_e(t) = P_e(0)\cos^2(\omega t/2),$$

where $\omega = J_{st}/\hbar$, J_{st} is the exchange interaction. For simplicity let the hole does not relaxed during time τ_h and after this time suddenly loses its polarization. Each event of hole spin relaxation induced the decrease of the electron polarization (see Fig. 7). Since the exchange interaction between the electron and the hole is small, then the electron spin rotates by the small angle during time τ_h. Electron spin polarization at $t = \tau_h$ can be rewritten as
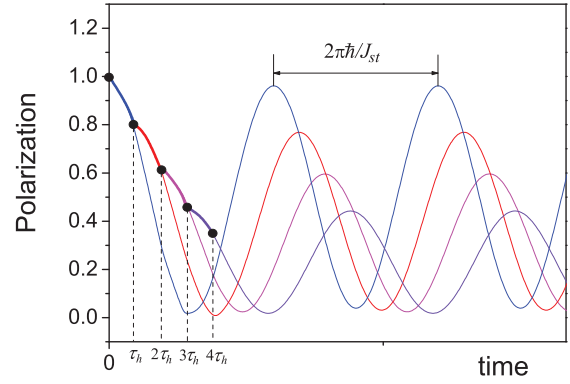
$$P_e(\tau_h) \approx P_e(0)(1 - (\omega\tau_h/2)^2).$$

FIG. 7. (Color online) Evolution of the electron polarization controlled by the exchange interaction with hole. τ_h is the characteristic time of the hole spin relaxation. Each event of hole spin relaxation induced the decrease of the electron polarization.

After N events of hole relaxation, electron polarization can be described by

$$P_e(N\tau_h) \approx P_e(0)\left((1 - \omega^2\tau_h^2)/4\right)^N$$
$$\approx P_e(0)\exp\left(-N\omega^2\tau_h^2/4\right).$$

For $t \gg \tau_h$ this expression turns into

$$P_e(t) = P_e(0)\exp(-t\omega^2\tau_h/4).$$

One can see therefore that the electron polarization P_e decays exponentially with the characteristic time,

$$\tau_e = 4/(\omega^2\tau_h) \equiv 4\hbar^2/\left(J_{st}^2\tau_h\right).$$

For estimation the time τ_e can be taken from ESR linewidth as 10^{-7} s. The time of hole relaxation can be taken two orders smaller (10^{-9} s), because the spin-orbit interaction constant in Ge is one order larger than the one in Si, and the mechanism of spin relaxation is the same as for electrons without illumination (the Dyakonov-Perel mechanism in the hopping regime).[23] As result, one can obtain $J_{st} \approx 0.1$ μeV.

Generally, this result can be useful in the development of new methods of extracting the information about spin states of holes localized in QDs. Electron spin states can serve as probes indicating the state of hole localized in Ge/Si QDs.

C. ESR results for double QD structure with spacer $d = 3$ nm

ESR study of QD structures with $d = 3$ nm gives the ESR signal consisting of two ESR lines. In the magnetic field applied along the growth direction these ESR lines have g factors of $g = 1.9994 \pm 0.0001$ and $g = 2.0002 \pm 0.0001$ (Fig. 8). The first ESR line (shown in Fig. 8 by the green dashed line) has the g-factor orientation dependence that is typical for electrons localized at the apexes of Ge QDs.[6] In the magnetic field applied along the growth direction of the structure the g factor of this ESR line practically coincides with the value of $g_\parallel$ in Si, and in perpendicular magnetic field the corresponding g factor $g = 1.9985 \pm 0.0001$ almost coincides with $g_\perp$ in Si. Orientation dependence of the g factor corresponds to localization of electrons in the Δ^{001} ($\Delta^{00\bar{1}}$) valleys (Fig. 4, blue circles) and coincides with one reported earlier.[6] The second ESR line (shown in the Fig. 8 by blue dotted line) has a rather
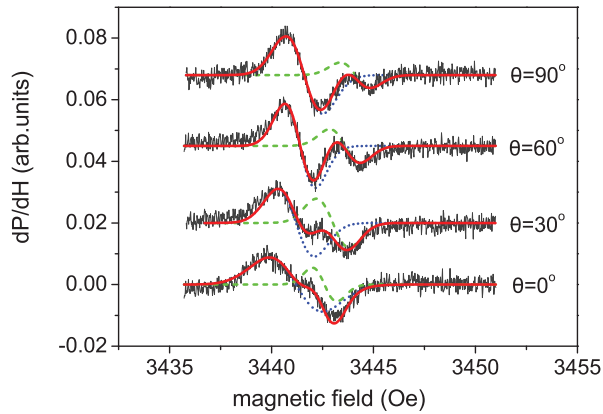
FIG. 8. (Color online) ESR spectra of electrons localized in the structure with double vertically aligned Ge/Si QDs, the distance between QDs layers $d = 3$ nm. For $\theta = 0°$ magnetic field is applied along the growth direction of nanostructure. Solid red line is approximation by the sum of two Gaussian lines. Dashed green and dotted blue lines present the components of this approximation. $\nu = 9.63381$ GHz, $T = 4.5$ K, microwave power $P = 0.063$ mW.

FIG. 9. (Color online) Wave function of the ground electron state calculated for the structure with $d = 3$ nm and $b = 3$ nm. Section of the YZ plane passing through the center of the long base edges of the QDs (left panel), section of the XZ plane passing through the center of the short base edge of the QDs (right panel). Scales along different axes differ.

small change of g factor with magnetic field direction; the in-plane magnetic field its g factor is $g = 2.0000 \pm 0.0001$. This ESR line has a g factor value typical for two-dimensional electrons in Si.[24]

As concerning ESR linewidth, this parameter does not change strongly with the magnetic field orientation. The ESR linewidth of the first signal is $\Delta H_{pp} \approx 1.2$ Oe at $\theta = 0°$, and at in-plane magnetic field it is $\Delta H_{pp} \approx 1.4$ Oe. In the previous study of electron states localized in the dense tunnel-coupled Ge quantum dot arrays the ESR linewidth changed four times, $\Delta H_{pp} \approx 0.8$ Oe at $\theta = 0°$, $\Delta H_{pp} \approx 3$ Oe at $\theta = 90°$.[6] The absence of such pronounced broadening in the present study can be explained by its compensation by ESR line narrowing, which is discussed in the beginning of Sec. III. The similar narrowing occurs for the second ESR line, its linewidth at $\theta = 0°$ is $\Delta H_{pp} \approx 2.5$ Oe, and for the in-plane magnetic field it is $\Delta H_{pp} \approx 1.8$ Oe.

To understand these results we calculate the energy spectrum in the effective mass approximation for the model structure with $d = 3$ nm. Calculations show that the ground state in this structure was formed by electron states corresponding to Δ^{001} and $\Delta^{00\bar{1}}$ valleys. Electrons are localized near the apexes of Ge QDs in upper layer of the structure (see Fig. 9) that has to provide ESR signal with g factor $g = 1.9994$ (at $\theta = 0°$).[6] The second ESR signal is attributed to the electrons localized near the lowest smooth boundary of the double QD layer. Localization of these electrons in XY directions is very weak. Results of calculation (without including of Coulomb interaction with impurity ions) show that their energy levels are found near the conduction band edge with the binding energy ~ 1 meV. Narrowing of the corresponding ESR line suggests that the localization of these electrons is enhanced by the external magnetic field applied perpendicularly to the plane of QD layers. With deviation of the magnetic field from the growth direction Z electrons become almost delocalized in two-dimensional plane that leads to the motional narrowing of the second ESR line. Narrowing of the first ESR line is also
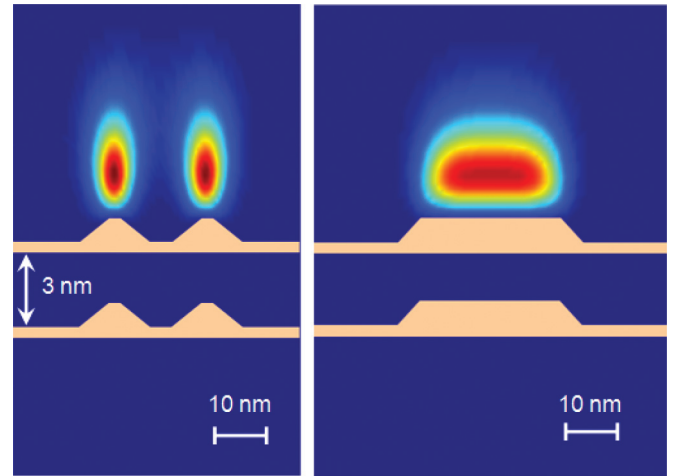
possible because for electrons localized at the QD apexes, more exactly, at the top edges of the QDs, the radius of localization is nearly the size of the QD (see Fig. 9, right panel) and correspondingly the magnetic length λ. In these conditions the localization radius can be changed by the external magnetic field through the shrinking of wave function tales. Then the narrowing has to happen also for the first ESR line. So, for both ESR lines the narrowing occurs, but for the first ESR line it is not so effective due to the competition with the opposite effect of ESR line broadening.

D. Electrons delocalized in the spacer between QD layers

QD structure with $d = 4$ nm demonstrates only one ESR line with a practically isotropic g factor, $g = 1.9992 \pm 0.0001$. A change of the g factor value with rotation of the sample in a magnetic field does not exceed the experimental accuracy of the measurements. This signal is related to electrons inside the Si layer between the QD layers. The effective accumulation of the strain from neighboring QD layers does not take place in this structure because of a larger distance between the QD layers. More weak strain cannot provide effective localization of electrons in the XY directions, and then electrons are practically delocalized in the Si layer between the QD layers, which is confirmed by the isotropic g factor. It is well known that delocalized electrons in heavily doped Si have the isotropic g factor $g = 1.9987$.[11] However, recently another g factor value $g = 1.9995$ was obtained for electrons at the conduction band edge.[25] Young *et al.* proposed some phenomenological dependence of the g factor on the binding energy of the electron states. Following this dependence the g factor $g = 1.9992$ corresponds to the binding energy near 10 meV. Perhaps in our case the weak localizing potential induced by Ge QDs in Si surroundings provides formation of shallow electron states near conduction band edge with a large localization radius. Conductivity in the sample can be realized by means of electron transitions between these states.
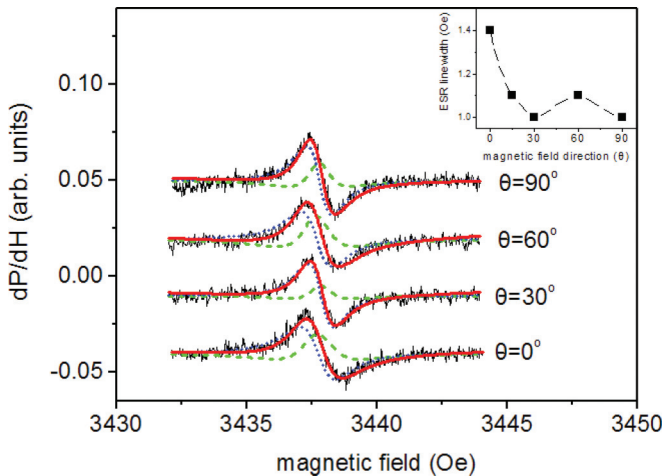
FIG. 10. (Color online) ESR spectra of electrons localized in the structure with double vertically aligned Ge/Si QDs, the distance between QDs layers $d = 4$ nm. The solid line represents the sum of an absorption line (dotted), and a dispersion line (dashed). The magnetic field is directed along the growth direction of the nanostructure for $\theta = 0°$ and perpendicular to this direction for $\theta = 90°$, $\nu = 9.61975$ GHz, $T = 4.5$ K, microwave power $P = 0.063$ mW.

Disappearance of the g-factor anisotropy can be explained by the averaging between strained and unstrained Si regions due to the large electron localization radius as well as by intervalley scattering in the case of fully delocalized carriers. Also the penetration of the electron wave function under the GeSi barrier can affect the electron g-factor value, resulting in the observed g factor $g = 1.9992$.[6]

The ESR linewidth changes only at the initial stage of the angular dependence, in the range $\theta \in \{0° \div 30°\}$. The ESR line is narrowed from $\Delta H_{pp} \approx 1.4$ Oe to $\Delta H_{pp} \approx 1$ Oe and then remains practically the same at all other orientations of the magnetic field. The ESR lines have the asymmetrical line shape, close to the Dysonian line shape (Fig. 10). This line shape has been observed earlier for two-dimensional electrons in SiGe/Si/SiGe quantum well structures[24] and for electrons in QD structures with large localization radius near to metal-insulator transition.[16] The origin of this asymmetry is the appearance of the dispersion signal due to the presence of conductivity in the system.

V. CONCLUSIONS

In conclusion, the localization of electrons in different Δ valleys in heterostructures with Ge/Si quantum dots was predicted theoretically and confirmed experimentally. It was demonstrated that the strain in Ge/Si QD multilayered structures can be used for electron g-factor engineering. A direct connection between g-factor value and spatial localization of electrons in QD structures was established. The effect of light-induced ESR line broadening was observed and explained by the electron-hole exchange interaction.

*aigul@isp.nsc.ru

[1] T. D. Ladd, F. Jelezko, R. Laflamme, Y. Nakamura, C. Monroe, and J. L. O'Brien, Nature **464**, 45 (2010).

[2] F. A. Zwanenburg, A. S. Dzurak, A. Morello, M. Y. Simmons, L. C. L. Hollenberg, G. Klimeck, S. Rogge, S. N. Coppersmith, and M. A. Eriksson, Rev. Mod. Phys. **85**, 961 (2013).

[3] A. I. Yakimov, A. V. Dvurechenskii, A. I. Nikiforov, A. A. Bloshkin, A. V. Nenashev, and V. A. Volodin, Phys. Rev. B **73**, 115333 (2006).

[4] A. F. Zinovieva, A. V. Dvurechenskii, N. P. Stepina, A. I. Nikiforov, A. S. Lyubin, and L. V. Kulik, Phys. Rev. B **81**, 113303 (2010).

[5] D. K. Wilson and G. Feher, Phys. Rev. **124**, 1068 (1961).

[6] A. F. Zinovieva, A. V. Dvurechenskii, N. P. Stepina, A. S. Deryabin, A. I. Nikiforov, R. M. Rubinger, N. A. Sobolev, J. P. Leitao, and M. C. Carmo, Phys. Rev. B **77**, 115319 (2008).

[7] Yu. N. Morokov, M. P. Fedoruk, A. V. Dvurechenskii, A. F. Zinov'eva, and A. V. Nenashev, Semiconductors **46**, 937 (2012).

[8] B. Voigtländer, Surf. Sci. Rep. **43**, 127 (2001).

[9] A. V. Nenashev and A. V. Dvurechenskii, J. Exp. Theor. Phys. **91**, 497 (2000).

[10] D. Grützmacher, T. Fromherz, C. Dais, J. Stangl, E. Mu1ler, Y. Ekinci, H. H. Solak, H. Sigg, R. T. Lechner, E. Wintersberger, S. Birner, V. Holy, and G. Bauer, Nano Lett. **7**, 3150 (2007).

[11] L. M. Roth, Phys. Rev. **118**, 1534 (1960).

[12] A. Stesmans and G. van Gorp, Rev. Sci. Instrum. **60**, 2949 (1989).

[13] Z. Wilamowski, W. Jantsch, H. Malissa, and U. Rössler, Phys. Rev. B **66**, 195315 (2002).

[14] Y. A. Bychkov and E. I. Rashba, J. Phys. C **17**, 6039 (1984).

[15] B. I. Shklovskii and A. L. Efros, *Electronic Properties of Doped Semiconductors* (Springer, Berlin, 1984).

[16] A. F. Zinovieva, N. P. Stepina, A. I. Nikiforov, A. V. Nenashev, A. V. Dvurechenskii, L. V. Kulik, N. A. Sobolev, and M. C. Carmo, arXiv:1311.2383 [cond-mat.mes-hall].

[17] M. I. D'yakonov and V. I. Perel', Sov. Phys. Solid State **13**, 3023 (1972).

[18] B. I. Shklovskii, Phys. Rev. B **73**, 193201 (2006).

[19] C. P. Slichter, *Principles of Magnetic Resonance* (Springer-Verlag, Berlin, 1978).

[20] A. I. Yakimov, A. V. Dvurechenskii, N. P. Stepina, A. V. Nenashev, and A. I. Nikiforov, Nanotechnology **12**, 441 (2001).

[21] A. I. Yakimov, A. A. Bloshsin, and A. V. Dvurechenskii, Appl. Phys. Lett. **93**, 132105 (2008).

[22] V. Zarifis and T. G. Castner, Phys. Rev. B **57**, 14600 (1998).

[23] A. F. Zinovieva, A. V. Nenashev, and A. V. Dvurechenskii, Phys. Rev. B **71**, 033310 (2005).

[24] Z. Wilamowski and W. Jantsch, Phys. Rev. B **69**, 035328 (2004).

[25] C. F. Young, E. H. Poindexter, G. J. Gerardi, W. L. Warren, and D. J. Keeble, Phys. Rev. B **55**, 16245 (1997).